Memory in a magnetic nanoparticle system: Polydispersity and interaction effects

S. Chakraverty,[1] M. Bandyopadhyay,[1] S. Chatterjee,[2] S. Dattagupta,[1] A. Frydman,[3] S. Sengupta,[1] and P. A. Sreeram[1]
[1]*Nano Science Unit, S. N. Bose National Centre for Basic Sciences, JD Block, Sector III, Salt Lake City, Kolkata 700098, India*
[2]*Department of Physics, University College of Science and Technology, Rajabazar Prangan, Kolkata 700009, India*
[3]*Department of Physics, Bar Ilan University, Ramat Gan 52900, Israel*
(Received 18 June 2004; revised manuscript received 1 November 2004; published 2 February 2005)

We report here a theory of relaxation of single domain magnetic nanoparticles, appropriate for analyzing measurements of Mössbauer spectra, magnetization response, and hysteretic coercivity. Our special focus of attention in the theoretical formulation is the presence of dipolar interaction between the magnetic particles. We discuss in detail the effect of interaction as well as particle size distribution on the measured relaxation spectra and irreversible, nonequilibrium magnetization response in field-cooled and zero-field-cooled situations. Some of the memory effects, similar to those seen in spin glass systems, may be put to important device applications by tuning the interaction and the particle size.

DOI: 10.1103/PhysRevB.71.054401 PACS number(s): 75.60.−d, 75.75.+a, 75.50.Lk, 75.50.Tt

I. INTRODUCTION

The subject of how a bulk magnetic specimen acquires a single domain structure and exhibits magnetic viscosity due to Néel relaxation, when its size is reduced, is an old one.[1–3] When the relaxation time τ is smaller than the measurement time, the specimen shows superparamagnetic behavior whereas in the opposite limit, relaxation is arrested. The crossover mark, derived from the temperature dependence of τ, yields the concept of "blocking temperature" (T_B). When $T<T_B$, one has a frozen moment, whereas for $T>T_B$, one sees magnetic viscosity. Thus single-domain magnetic particles have been a happy hunting ground for studying nonequilibrium phenomena, characterized by irreversibility, hysteresis and other memory effects.

In recent times this subject has attracted a great deal of attention in view of the heightened interest in nanoscience and magnetic memory devices. As it turns out, it is not just the temperature T which can be used as a control parameter but even the mean size and the distance between the particles can be profitably tuned because of the exponential dependence of τ on the volume (V) of the particle.[4–10] Thus polydispersity leads to a distribution of relaxation times,[11,12] those larger than the measurement time yielding "frozen" behavior, and those shorter giving rise to "magnetic viscosity."[9,10] A given sample then displays strong memory effects, which are reported here. Our results are based on the measurements of temperature-dependent magnetization during cooling and heating cycles. These memory effects may have important device applications in the future.[6] In this paper we report the theory of relaxation, relevant to Mössbauer, magnetization and coercivity measurements, and back up our theory results with qualitative comparison with our experimental data.

The system we employ for our experimental investigation is nickel ferrite particles ($NiFe_2O_4$) embedded in a host nonmagnetic SiO_2 matrix. We prepared the following two specimen samples by using the sol-gel technique:[13] Sample A, which contains (35%) $NiFe_2O_4$ (by volume), making possible a weak dipolar interaction between the magnetic particles, and Sample B, which contains (15%) $NiFe_2O_4$, believed to yield a noninteracting case. The phase of the samples was identified by x-ray diffraction.[14] Both x-ray photographs and TEM micrographs suggest that the mean interparticle separation is 5 nm for specimen A and is 15 nm for specimen B, whereas for each specimen the average particle radius is $\approx$3 nm.

With the preceding background the paper is organized as follows. In Sec. II we review the basic relaxation theory of single-domain magnetic particles and specialize to the case of large uniaxial anisotropy *vis-a-vis* the thermal energy. In this limit the relaxation dynamics can be described in terms of a two-state rate theory. We motivate next a mean field theory in order to incorporate a *weak* dipolar interaction between the magnetic particles. The assumption of the weakness of the dipolar coupling is checked by the measured hysteresis loop. The theory developed in Sec. II is employed to interpret the Mössbauer data for specimens A and B, presented in Sec. III. The main point of Sec. III is to underscore the issue that even though the interaction does not lead to magnetic order, it can slow down relaxation, even at the highest (room) temperature of measurement. Section IV is the core of the paper in which we demonstrate how memory effects can arise due to polydispersity of the sample and how these effects can be tamed by the effects of interaction. The observed memory effects are similar to those reported in Ref. 11. But unlike Ref. 11 which attributes the data to spin glass interactions, our interpretation is quite different in that the effects simply occur due to a superposition of different response functions with at least one short and one long relaxation times compared to the observation time. Finally, in Sec. V we present our main conclusions about the significance of the reported results.

II. RELAXATION THEORY

We assume for the sake of simplicity that the anisotropy, responsible for single-domain behavior of the magnetic nanoparticle is uniaxial, governed by the energy,

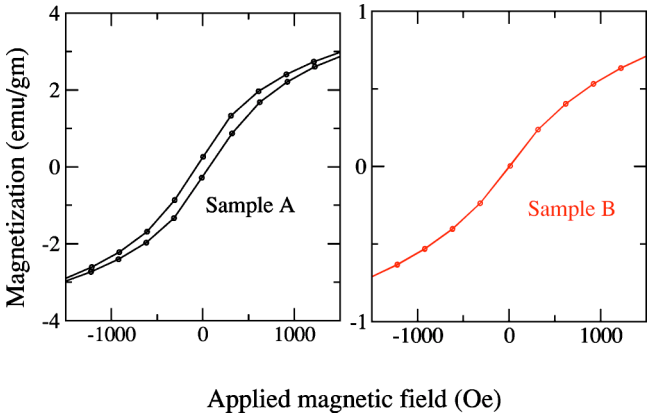

FIG. 1. Room temperature dc *M-H* measurement of interacting sample A and noninteracting sample B. The solid lines are drawn through the experimental points, indicated by dots.

$$E(\Phi) = VK \sin^2 \Phi. \tag{1}$$

In Eq. (1), V is the volume of the particle, K is a parameter referred to in the literature as the anisotropy energy, and Φ is the angle between the anisotropy axis and the direction of the "giant" magnetic moment of the single-domain particle. Because of thermal fluctuations the magnetic moment undergoes rotational Brownian motion over an anisotropy barrier in Eq. (1), in which $\Phi(t)$ is a continuous stochastic process as a function of the time t.[15] However it turns out that if $VK \gg K_B T$, K_B being the Boltzmann constant and T is the absolute temperature, the magnetic moment is mostly locked in two orientations, corresponding to $\Phi = 0$ and $\Phi = \pi$, with slow relaxation between the two configurations. Thus we are in the so-called "Ising" limit in which $\Phi(t)$ may be viewed as a dichotomic Markov process, in which it jumps at random between the angles 0 and π at a rate governed by the Arrhenius-Kramers formula,

$$\lambda_{0\to\pi} = \lambda_{\pi\to 0} = \lambda_0 \exp\left(-\frac{KV}{K_B T}\right), \tag{2}$$

where λ_0 is the "attempt" frequency. In what follows we restrict our discussion to the Ising case wherein the magnetic moment vector points either parallel or antiparallel to the anisotropy axis.

We now discuss the effect of interaction which, for the present system at hand in which the magnetic particles are embedded in a dielectric host (SiO_2) matrix, is surmised to be of dipolar in nature. It is well known that dipolar interactions, being long-ranged, anisotropic and alternating in the sign of interaction, can indeed lead to very complex magnetic order.[16] However, our dc *M-H* measurement, exhibited in Fig. 1, indicates that even for specimen A for which the dipolar interaction is relevant, there is no shift of the hysteresis loop, thereby implying that the bulk magnetization, for the zero applied field, is *zero*. Our interpretation is that because of the largeness of anisotropy energy as mentioned above, we are operating in the Ising limit of the dipolar interaction, for which the local field, in the mean field sense, points parallel or antiparallel to the anisotropy axis, with equal probability. The dipolar coupling can now be described by its "truncated" form[17]

$$\mathcal{H}_{d-d} = \sum_{ij} \gamma_i \gamma_j \hbar^2 \frac{(1 - 3\cos^2\theta_{ij})}{|\vec{r}_{ij}|^3} m_{zi} m_{zj}, \tag{3}$$

where γ_i and γ_j are the gyromagnetic ratio of the ith and jth particle, respectively, $\vec{r}_{ij}$ is the vector distance between the "sites" at which the two magnetic particles are located, θ_{ij} is the angle between $\vec{r}_{ij}$ and the anisotropy axis and m_{zi} is the (giant) magnetic moment for the ith nanoparticle along the direction of anisotropy axis (i.e., Z). Given the fact that m is proportional to the volume V of the particle, Eq. (3) can be rewritten as

$$\mathcal{H}_{d-d} = \mu^2 V^2 \sum_{ij} \gamma_i \gamma_j \hbar^2 \frac{(1 - 3\cos^2\theta_{ij})}{|\vec{r}_{ij}|^3} \cos\Phi_i \cos\Phi_j, \tag{4}$$

where μ is the magnetic moment per unit volume and Φ has the same definition as in Eq. (1). The interaction in Eq. (4), along with that given in Eq. (1), is quite complicated to treat in detail. For the purpose of this paper we invoke a mean field theory in which each magnetic nanoparticle is visualized to be embedded in an effective medium which creates a local magnetic field at its site. Thus in this approximation, $\mathcal{H}_{d-d}$ is replaced by its mean field (MF) form

$$\mathcal{H}^{\mathrm{MF}}_{d-d} = \gamma\hbar\mu^2 V^2 \cos\Phi \sum_{j} \gamma_j \hbar \frac{(1 - 3\cos^2\theta_{ij})}{|\vec{r}_{ij}|^3} \langle \cos\Phi_j \rangle, \tag{5}$$

wherein the angular brackets $\langle \cdots \rangle$ represent a thermal average. Further, in accordance with our assumption about the largeness of the anisotropy energy, $\cos\Phi$ can be replaced by a two-state Ising variable σ,

$$\mathcal{H}^{\mathrm{MF}}_{d-d} = \gamma\hbar\mu^2 V^2 \sigma \sum_{j} \gamma_j \hbar \frac{(1 - 3\cos^2\theta_{ij})}{|\vec{r}_{ij}|^3} \langle \sigma_j \rangle, \tag{6}$$

In line with this approximation each particle can be viewed to be subjected to a local magnetic field H such that

$$\mathcal{H}^{\mathrm{MF}}_{d-d} = \mu V \sigma H, \tag{7}$$

$$H = \mu \Lambda V \langle \sigma \rangle, \tag{8}$$

where Λ is a parameter that subsumes all the other constants. Note that we have dropped the suffix j on σ, implying that we consider the embedding medium to be homogeneous. Within the proposed self-consistent mean field theory, H can be expressed as

$$H = \mu \Lambda V \tanh\left(\frac{\mu V H}{K_B T}\right). \tag{9}$$

Note that Eq. (9) admits both positive and negative solutions for H, in accordance with our discussion preceding Eq. (3). Further, within the present approximation in which Φ is restricted to the value 0 and π, the anisotropy energy in Eq. (1) does not figure in the expression for H. We now turn our attention to relaxation kinetics. The dichotomic Markov process, mentioned in the paragraph preceding Eqs. (3) and (4), yields the following set of rate equations for the number of

magnetic particles with a specific orientation of their magnetization:

$$\frac{d}{dt}n_0(t) = -\lambda_{0\to\pi}n_0(t) + \lambda_{\pi\to 0}n_\pi(t), \tag{10}$$

$$\frac{d}{dt}n_\pi(t) = \lambda_{0\to\pi}n_0(t) - \lambda_{\pi\to 0}n_\pi(t), \tag{11}$$

where the subscripts on n indicate the two allowed values of Φ. Solving Eqs. (10) and (11), we may derive for the time-dependent magnetization $M(t)$:

$$M(t) \equiv V\mu[n_0(t) - n_\pi(t)] = M(t=0)\exp(-\bar{\lambda}t) + \mu VN\frac{\Delta\lambda}{\bar{\lambda}}[1-\exp(-\bar{\lambda}t)]. \tag{12}$$

In Eq. (12),

$$N = n_0 + n_\pi, \tag{13}$$

which is a constant,

$$\bar{\lambda} = \lambda_{0\to\pi} + \lambda_{\pi\to 0} \tag{14}$$

and

$$\Delta\lambda = \lambda_{\pi\to 0} - \lambda_{0\to\pi}. \tag{15}$$

The expressions for the rate constants necessitate now a generalization of Eq. (2) in view of the dipolar interaction, and are given by

$$\lambda_{0\to\pi} = \lambda_0\exp\left(-\frac{V(K+H\mu)}{K_BT}\right), \tag{16}$$

$$\lambda_{\pi\to 0} = \lambda_0\exp\left(-\frac{V(K-H\mu)}{K_BT}\right), \tag{17}$$

wherein we have neglected terms of order H^2/K^2. We conclude this section by reiterating a few remarks on the theory presented here. First, we have assumed at the outset that the anisotropy is large, a very good assumption in the context we believe, which has allowed us to approximate a continuous stochastic process by its discrete version. The anisotropy barrier does not appear in equilibrium properties [cf. Eq. (9)] but does strongly influence relaxation kinetics [cf. Eqs. (16) and (17)]. Our second remark concerns the dipolar interaction, which is treated in mean field theory. This interaction, though weak, has a significant contribution to the relaxation effects [cf. Eqs. (16) and (17)]. In particular, and in the context of magnetic nanoparticles, the relaxation rates acquire a V^2-dependent term in the exponent [see also Eqs. (8) and (9)] in addition to an effective temperature-dependent tanhyperbolic term. The effect of this contribution is found to be of profound importance in interpreting our data on irreversible magnetization, as presented in Sec. IV below.

III. INTERACTION EFFECT ON MÖSSBAUER SPECTRA

In this section we present our experimental results on Mössbauer spectroscopy and interpret them in the light of the theory given in Sec. II. We will show that the dipolar interaction, though weak, yields a static-looking Mössbauer spectra, because of a time-window effect. The measurement technique is based on the absorption of a 14.4 keV gamma ray transition from the excited nuclear level of angular momentum $I=\frac{3}{2}$ to the ground level of $I=\frac{1}{2}$.[18] In a static magnetic field the levels are split, giving rise to the characteristic six-finger pattern. On the other hand, when the field fluctuates in time rapidly around a zero mean the spectrum collapses to a single line, as though there were no magnetic field. It is important at the outset to grasp what exactly the measurement time is as far as Mössbauer spectroscopy is concerned.[19] It might seem it is the nuclear lifetime τ_N at first sight, but in point of fact the measurement time-window is provided by the inverse of the Larmor frequencies (associated with the Zeeman interaction) that determine the line positions of the six-finger pattern.[20] When the frequencies are larger than the relaxation rate τ one sees a static pattern whereas in the opposite limit the pattern collapses to a single line.

The observed Mössbauer spectra as a function of temperature for specimens A and B are shown in Figs. 2 and 3, respectively.[21] From the room temperature data in Fig. 2 it is evident that the effect of interaction slows down relaxation even at the highest T. We interpret the data based on the following stochastic model Hamiltonian:[22]

$$\mathcal{H}(t) = -\mu_N g(I) I_z h(t), \tag{18}$$

where μ_N is the nuclear magneton, $g(I)$ is the level-specific g-factor depending on whether the nucleus is in the excited or ground level, I_z is the component of the nuclear angular momentum along the Z-axis, that is determined by the anisotropy direction of the single-domain particle, and $h(t)$ is a local field at the nucleus that jumps about stochastically in time.

The local field $h(t)$ at the nucleus is of course produced by the magnetization of the particle which, for reasons mentioned earlier, is taken to jump between $\pm h_0$, where h_0 is proportional to H, at the rates given by Eqs. (16) and (17). The Mössbauer line shape as a function of frequency ω is given by[22]

$$I(\omega) = \frac{1}{\pi}Re\sum_{m_0m_1}|\langle I_0m_0|A|I_1m_1\rangle|^2\int dVf(V) \times\left[\left(-i\omega+\frac{\Gamma}{2}\right)+\frac{\mu_N^2h_0^2(g_0m_0-g_1m_1)^2}{\left(-i\omega+\frac{\Gamma}{2}\right)+\bar{\lambda}(V)/2}\right]^{-1}. \tag{19}$$

In Eq. (19) A is the nuclear transition operator, the matrix elements of which are given by Clebsch-Gordan coefficients, Γ is the natural linewidth of the excited nuclear level, $g_0(g_1)$ is the g-factor in the ground (excited) level and $\bar{\lambda}(V)$ is the volume-dependent relaxation rate as given in Eq. (14). The integral over V incorporates the particle size distribution with the aid of a probability function $f(V)$,[8,23]

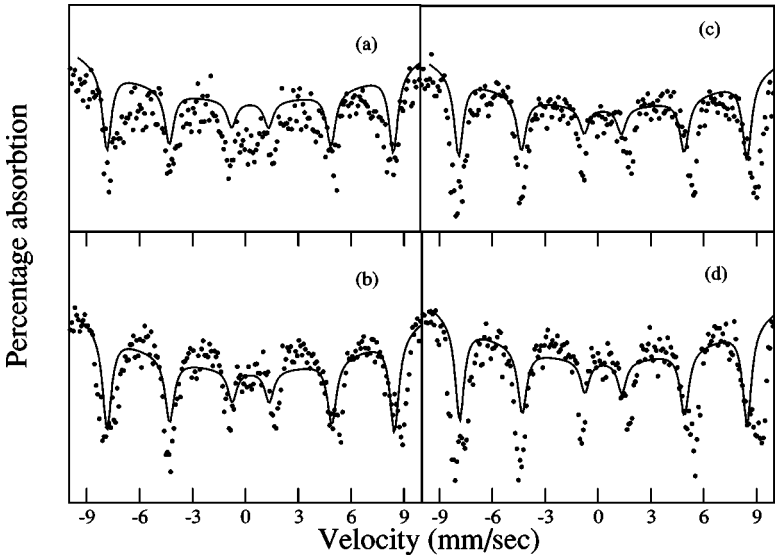

FIG. 2. Temperature-dependent Mössbauer spectra of sample A, dots are the experimental points and solid lines are the curves fitted from our model, (a) room temperature, (b) 220 K, (c) 100 K, (d) 20 K.

$$f(y) = \frac{1}{ys\sqrt{2\pi}} \exp\left[- \frac{\left(\log \frac{y}{y_0} \right)^2}{2s^2} \right], \qquad (20)$$

where y is the particle diameter, y_0 is the most probable diameter, and s controls the width of the distribution. For numerical calculation we have taken $y_0 = 3$, $s = 1.8$, $KV = 10^{-13}$ erg, and $\mu = 100$ emu/g. From the fitting of the Mössbauer sepctra (Figs. 2 and 3) the values of the relaxation rate λ are computed, which are reproduced in Tables I and II. Since there is a volume distribution [cf. Eq. (20)] there will also be a distribution of the relaxation rate λ. In Figures 2 and 3 those values of λ which correspond to fast relaxation yield a broad central line, which provides a background to the split spectra. This background is eliminated in our fitting procedure and what appears in Tables I and II is an estimated λ, from Eq. (19) by ignoring $f(V)$. As expected, λ for a given temperature is systematically smaller for the interacting case (sample A) than for the noninteracting case (sample B) in view of the quadratic volume dependence in the exponent, as mentioned at the end of Sec. II. Further, the strong volume dependence makes λ rather insensitive to temperature variations below 200 K for the interacting sample (A) (cf. Table II).

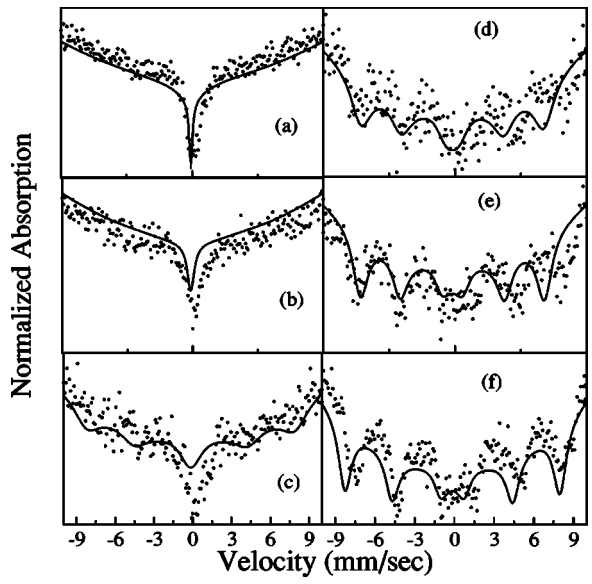

FIG. 3. Temperature-dependent Mössbauer spectra of sample B, dots are the experimental points and solid lines are the curves fitted from our model, (a) room temperature, (b) 250 K, (c) 200 K, (d) 125 K, (e) 50 K, (f) 20 K.

Coming back to Fig. 2, we note that the spectra are indicative of the presence of an internal magnetic field which is apparently static. We surmise that this internal field has its origin in the dipole-dipole interaction between magnetic particles, when their mean separation is around 5 nm. As we discussed earlier in Sec. II and at the end of the paragraph above, the observed six-finger structure throughout the entire temperature regime is not due to any spontaneous magnetization but a time-window effect as borne out in Tables I and II. This happens due to the fact that the mean dipolar field, as mentioned earlier, is equally probable to point along $+Z$ and $-Z$ direction and keeps fluctuating between these two possibilities.

Given this background to our theoretical analysis, the interpretation of Mössbauer spectra as shown in Figs. 2 and 3, is as follows. At any given point in time, half of the Mössbauer nuclei find their "local" magnetic field pointing along $\Phi = 0$ while the other half will see the local field pointing

TABLE I. Fitted values of the relaxation rate λ obtained from the Mössbauer spectra as a function of temperature for the noninteracting sample B.

Temperature (K)	λ (mm/s)	Error (± mm/s)
21	2.44	0.22
125	2.96	0.41
200	10.62	0.53
250	10.84	0.60

TABLE II. Fitted values of the relaxation rate λ obtained from the Mössbauer spectra as a function of temperature for the interacting sample A.

Temperature (K)	λ (mm/s)	Error (±mm/s)
20	1.36	0.18
100	1.34	0.12
200	1.36	0.10
250	1.74	0.07
300	2.05	0.11

along $\Phi=\pi$. Both these orientations of the local field would of course yield an identical six-finger pattern, because the nucleus as an observer cannot distinguish between $\Phi=0$ and $\Phi=\pi$, provided the local field is static, within the Mössbauer measurement time. That of course is determined by the temperature T and the mean dipolar strength parametrized by Λ. These two quantities determine the rates of relaxation of the local dipolar field, as indicated in Eqs. (16) and (17). Hence for sample B, for which the dipolar field is negligible, semblance of a six-finger pattern shows up only at the lowest T when relaxation slows down, whereas for sample A, the dipolar coupling keeps the relaxation slow within the nuclear time-window, at all temperatures.

IV. POLYDISPERSITY-LINKED MEMORY EFFECTS

Having discussed the effect of slowing down of relaxation due to the weak interaction between magnetic nanoparticles, both in terms of theory in Sec. II, corroborated by Mössbauer experiments in Sec. III, we focus our attention to another important attribute, viz., the volume-distribution of the nanoparticles. We show that such a distribution leads to striking memory effects in our low-temperature dc magnetization measurements. Surprisingly the dipolar interaction, the subject of our discussion in Secs. II and III, suppresses the memory effects.

The magnetization measurements, are carried out in accordance with the following cooling and heating protocol. At $T=300$ K ($T=T_\infty$), a small magnetic field ($h=50$ Oe) is applied and the magnetization (M) measured. Keeping the field on, the temperature (T) is lowered continuously at a steady rate to T_n and M is simultaneously measured up to the temperature T_n. Thus one obtains M versus T in the cooling regime ($T_n \leqslant T \leqslant T_\infty$). At T_n the field is switched off and the drop of M is monitored for several (≈ 4) hours. Subsequently, the magnetic field is *switched* back on and $M(T)$ versus T is mapped in the cooling regime ($T_{n-1} \leqslant T \leqslant T_n$). At T_{n-1} the field is switched off again and the process of measurement repeated, until the lowest temperature T_0 is reached. Thus, one obtains field-cooled response and zero-field relaxation of the magnetization as a function of temperature. At the end of the cooling cycle, at T_0, the field is turned on and $M(T)$ monitored as the system is heated from T_0 through T_{n-2}, T_{n-1}, T_n and eventually to T_∞, the magnetic field remaining on throughout. Our results are shown in Fig. 4, for sample A and sample B. The heating path surprisingly shows wiggles in $M(T)$ at all the T steps T_{n-2}, T_{n-1}, T_n where h was earlier switched off during cooling, apparently retaining a memory of the temperature steps at which the cooling was arrested. One tantalizing aspect of our results is that memory effects are more prominent for sample B than for sample A, although in the latter the average interparticle distance is smaller and hence the dipolar interaction non-negligible. Recently Sun *et al.*[11] have reported very similar history dependent effects in the magnetization measurements of a monolayer of sputtered permalloy ($Ni_{81}Fe_{19}$) clusters on a SiO_2 substrate. These authors attribute the disparate cooling and heating histories to aging and concomitant memory effects found in a spin glass phase.[24] Spin glass transitions are known to occur due to disorder and frustration in dilute magnetic alloys that are characterized by a complicated free energy landscape with deep valleys and barriers.[25] Strongly nonequilibrium memory dependent behavior ensues as a result of the system getting trapped in a deep valley such that the relaxation time (τ) for deactivation becomes long compared to experimental time scales of measurement.[26]

Our interpretation of the results shown in Fig. 4 is very different from that of Ref. 11. We demonstrate below that the observed phenomena are *not* connected to complicated spin glass type interactions but can be simply attributed to a superposition of relaxation times, arising from particle size distribution, as it were in *noninteracting* single-domain magnetic particles. Experimentally it is known[12] that nanoparticle sizes are usually distributed according to a log-normal distribution. However, we show below that the exact form of the distribution is irrelevant for explaining the memory effect. In fact, in order to keep the analysis simple and to obtain a clear

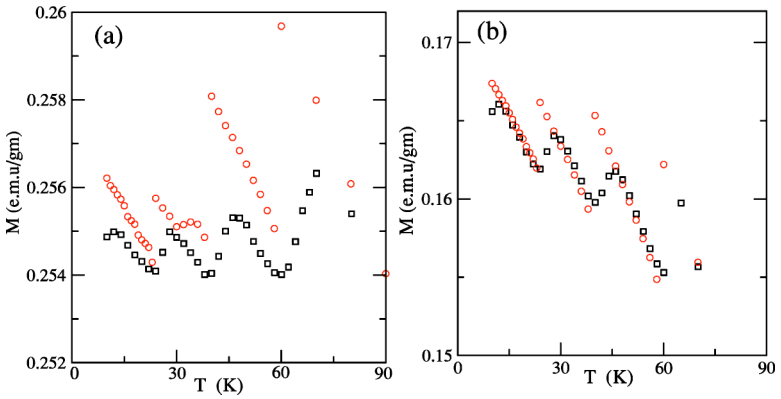

FIG. 4. (Color online) Experimental $M(T)$ curves during cooling (○ red) in a small magnetic field $h=50$ Oe and zero-field heating (□ black) for the (a) interacting and (b) noninteracting samples showing prominent memory effects. A constant heating/cooling rate of 2 K/min was maintained except at 60 K, 40 K, and 20 K where the cooling was arrested for 4 h duration at each temperature during which time h was switched off.

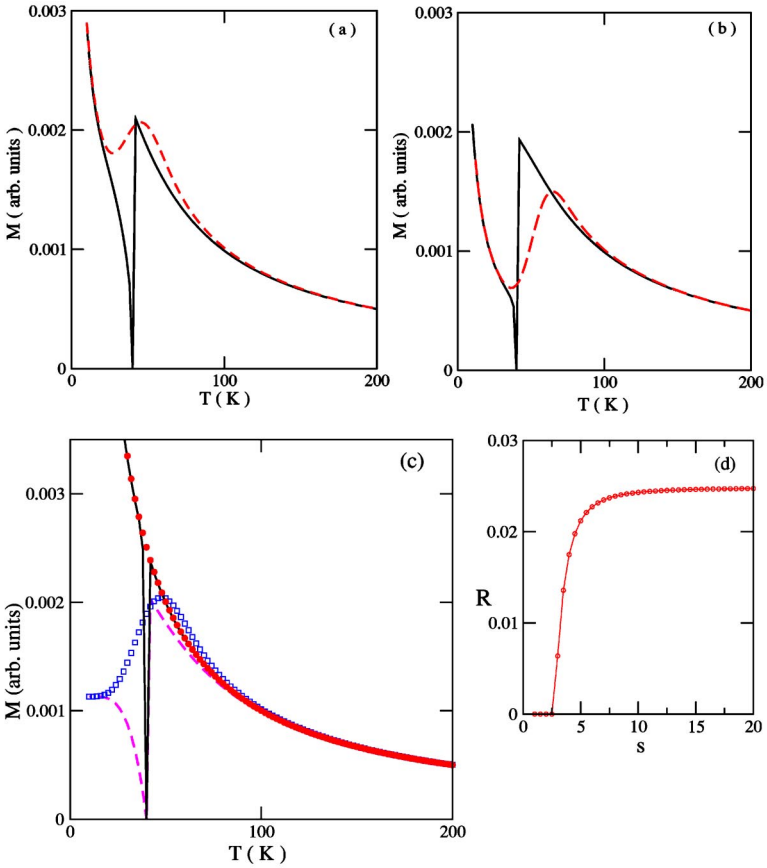

FIG. 5. (Color online) Simulated M (arbitrary unit) vs T curves during cooling (solid black) and heating (dashed red) for the (a) interacting and (b) noninteracting cases: The curve (c) shows the various contributions to the total magnetization of interacting sample A coming from the (i) fast particles during the cooling cycle (black solid line), (ii) fast particles during the heating cycle (red filled circle), (iii) slow particles during the cooling cycle (magenta dashed line), and (iv) slow particles during the heating cycle (blue square). The theoretical curves (a)–(c) have been calculated using a double delta function distribution of particle sizes. Curve (d) shows a plot of the recovery parameter R (see text) as a function of the width(s) of a Gaussian particle size distribution.

understanding of the physics it is sufficient to take a sample size distribution consisting of two delta function peaks so that there are only two kinds of particles "large" (volume V_1) and "small" V_2. Correspondingly we have only two relaxation times $\tau=\tau_1$ and τ_2 in our model, if we remember that [cf. Eqs. (16) and (17)],

$$\tau(V) \propto \exp\left[\frac{(KV \pm \mu HV)}{K_B T}\right]. \tag{21}$$

The interpretation of the observed results hinges on the premise that the time τ_1 is much larger than the measurement time while τ_2 is much smaller, at the lowest measured temperature (T_0). Both τ_1 and τ_2 are expected to be smaller than the measurement time at the highest temperature T_∞. Therefore, in the intermediate temperature domain ($T_0 \leqslant T \leqslant T_\infty$), the small particles equilibrate rapidly, thus showing superparamagnetic viscosity[10] while the large particles are "blocked." This is observed in Fig. 5(c) where we have plotted computer simulations of $M(T)$ separately for the two sets of interacting particles under the same cooling and heating regimens. Here we choose the temperature T^* at which h is switched off such that the blocking temperatures[8,9] corresponding to the two different particle sizes flank T^*. The simulations are based on rate theory calculation for the time dependent magnetization given in Sec. II. When h is zero, both sets of particles relax to $M=0$. However, when h is turned on, particles 1 are blocked ($M=0$) while particles 2 show facile response. As T is increased again, M for particles 2 decreases with T while M for particles 1 initially increases before dropping off. The resultant graph is a superposition [see Fig. 5(c)] of a monotonically decreasing curve and a hump, thus producing a wiggle. This effect is seen only when the temperature of arrest is in-between the two respective blocking temperatures, in conformity with the findings of Ref. 12. We have performed measurements on the same system but now with increased interparticle separation ($\simeq$15 nm) [see Fig. 4(b)], the simulation results of which are shown in Fig. 5(b).

The resultant interaction effect due to dipole-dipole coupling, not considered in Ref. 12, is also quite distinct from the quenched-in disorder mediated interactions proposed in Ref. 11. As described earlier the effect of interaction, within a mean-field picture, is incorporated by adding a term proportional to V^2 in the exponent of $\tau(V)$ [cf. Eqs. (8) and (9)]. Thus, even small particles (V_2) can now have τ_2 *larger* than the measurement time. This becomes more prominent at lower temperatures. Therefore, the blocking temperatures for both particles 1 and 2 are now shifted to higher T, thereby causing the wiggles to disappear. This is consistent with the results of Fig. 4 which show that the memory effects are *stronger* for the noninteracting particles. We conclude then that the unexpected wiggles seen in the cooling and heating cycles of $M(T)$ versus T have much less to do with interaction effects but more to do with polydispersity of the sample.

How crucially does the nature of the particle size distribution function affect the magnetization recovery during the zero field heating cycle? In order to answer this question we first quantify the memory effect by defining a parameter,

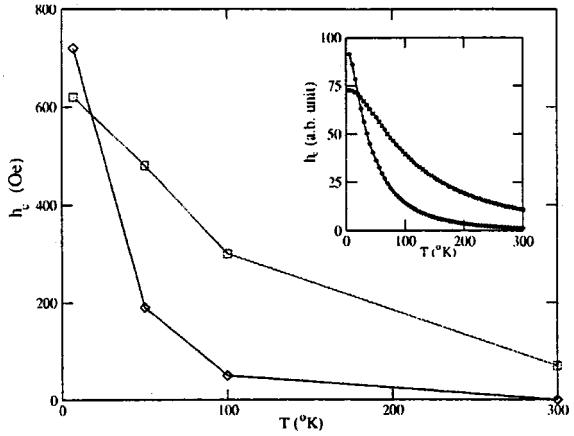

FIG. 6. (Color online) Coercivity (h_c) as a function of temperature for the interacting (□ red) and noninteracting (◇ black) samples. The corresponding curves (h_c in arbitrary units) obtained from our theory assuming a double delta function particle size distribution are shown in the inset.

$$R = \Theta\left(\left.\frac{dM}{dT}\right|_{T=T_n}\right)\frac{dM}{dT}, \tag{22}$$

where $\Theta(x)$ is the Heaviside step function. The parameter R measures the positive slope of the $M(T)$ curve during zero field heating. We have calculated R using a Gaussian size distribution centered at $V=V_0$ and with width s. Our results for R are shown in Fig. 5(d) for a particular choice of V_0 as a function of s. We observe that R increases with the width of the distribution and saturates quickly. In this regime, R is almost independent of V_0 and accordingly, the detailed nature of the distribution. We conclude that the memory effects will be best seen in samples with a dilute dispersion of particles but a very wide (flat) distribution of sizes. Indeed in this limit the relaxation is known to be prominently dominated by magnetic viscosity characterized by a logarithmic relaxation in time.[11] Not surprisingly, a logarithmic relaxation has been observed in the experiments of Sun *et al.* although the interpretation offered is different from ours.[11]

Our interpretation of the M vs T data is further substantiated by our earlier reported results (in Fig. 1) of hysteresis measurements and thereby coercivity estimation for both the interacting sample A and noninteracting sample B. Clearly, for sample B the relaxation times are shorter than the measurement time, at 300 K. Thus, there is no hysteresis loop and the coercivity (measured by the width along the abscissa on the zero-magnetization line) is also zero. On the other hand, for sample A, we observe a nonzero coercivity even at 300 K due to the slowing down of relaxation because of the presence of an additional term proportional to V^2 in the exponent of $\tau(V)$ as mentioned above.

Next we repeat the above measurements down to 4 K, using a SQUID magnetometer. The coercivity (h_c) is plotted as a function of temperature (T), in Fig. 6. Because relaxation slows down for both sample A and sample B, h_c increases with decrease of T (Fig. 6). The coercivity of the interacting sample A is larger than that noninteracting sample B for temperatures greater than 25 K. However, at $T=25$ K a surprising *crossover* is detected, where the coercivity for sample B shoots above that for sample A. We suggest that the reason for this behavior is that the term H in the exponent of $\tau(V)$ in Eq. (21) is replaced by $h+\delta H$, where h is the applied field and the mean field δH arises from interaction [cf. Eq. (9)]:

$$\delta H = \mu V \Lambda \tanh\left(\frac{\mu V(h+\delta H)}{K_B T}\right). \tag{23}$$

The tanh term augments the V^2 term in the exponent of $\tau(V)$ below 25 K, making the larger particles relax so slowly that they do not respond to H at all. Therefore, the larger particles are "frozen out" from further consideration, making the mean relaxation time in the interacting case even smaller than that for the noninteracting case. This somewhat nonintuitive conclusion is further confirmed by our simulated coercivity computation, shown in Fig. 6 (inset).

To verify our argument further we perform a separate set of experiments on both samples A and B as follows. We field-cool the samples down to 10 K from 300 K in the presence of $h=100$ Oe. At 10 K the magnetic field is switched off and the relaxation of the magnetization measured. We find that the average relaxation time obtained by forcing an exponential fit to our data of sample A is 100 min and that of sample B is 25 min We then heat the samples to 300 K, and cool it back down to 10 K at zero magnetic field. At 10 K we switch on the magnetic field and wait for 2 h. The magnetic field is then switched off and the magnetization measured. The relaxation time of sample B remains 25 min but the relaxation time of sample A decreases to 30 min. This result is consistent with the reasoning described in the above paragraph. Therefore, for the low-temperature interacting system, larger particles are rendered magnetically inactive. This result is a dramatic illustration of the interplay of polydispersity and interaction effect in determining the relaxation behavior of magnetic nanoparticles which is indeed the underpinning theme of the present paper.

V. SUMMARY AND CONCLUSION

The revival of interest in single-domain magnetic particles due to the resurgence of nanoscience and technology has spurred us to examine in detail the underlying relaxation phenomena. We have presented here both theoretical and experimental results and their intercomparison. Our main focus has been to analyze how the relaxation and response behavior of magnetic nanoparticles is influenced by their mutual interaction as well as polydispersity of particle sizes. The theory presented in Sec. II is based on the simplifying assumption of large uniaxial anisotropy energy vis-a-vis the thermal energy. A further simplifying assumption has been invoked in treating the interaction due to dipolar coupling between magnetic nanoparticles within a mean field approximation. A more complete treatment, requiring the full phase space dynamics of the underlying rotational relaxation of the particles and the need to consider arbitrary orientation of the magnetic field, both external and internal, with respect to

anisotropy axis, is a subject of ongoing investigation.[27] The simplified theory of Sec. II has been applied to the Mössbauer experiments, described in Sec. III. Mössbauer spectroscopy is a sensitive *local* tool, both in spatial sense as well as temporal sense. Thus it has been shown in Sec. III that even though the dipolar interaction does not lead to bulk magnetic order, it yields local order within the time-window of the Mössbauer measurement. This slowing down of the relaxation process, occasioned by interaction, has important consequence for memory effects. Memory effects have indeed been our primary focus of attention, further dealt with in Sec. IV. The symbiotic relationship of polydispersity and interaction in influencing the relaxation phenomena has been brought out through low-temperature magnetization and coercivity data. We have demonstrated that just a bimodal distribution of particle size, in which one set of particles remains frozen in its response behavior while the other set exhibits magnetic viscosity, suffices to interpret dramatic memory effects seen in cooling and heating cycles of the magnetic response. These memory effects are quite akin to and often interpreted to be due to much complex spin glass phenomenon which is characterized by fascinating aging effects. In conclusion, the strong history dependent effects seen in magnetization and coercivity measurements in $NiFe_2O_4$ magnetic nanoparticles have been interpreted as being due to arrested Néel relaxation. Our model has been simplified by choosing just two volumes of the particles, on either side of the "blocking" limit. Further corroboration of the proposed mechanism has been achieved by performing measurements on an interacting system. Our results suggest that either by tuning the interaction (through changing interparticle distance) or by tailoring the particle size distribution, these nanosized magnetic systems can be put to important application in memory devices. In particular, a flat volume distribution can be of greater utility than a monodispersed distribution with a single sharp peak.

ACKNOWLEDGMENTS

S.C. thanks Kalyan Mandal for guidance on sample preparation. M.B. acknowledges support from CSIR. A.F. would like to thank Israel Science Foundation Grant No. 326/02-3 for funding this work. S.S. acknowledges financial support from DST Grant No. SP/S2/M-20/2001. Finally, the authors acknowledge support from the Department of Science and Technology (DST) through its Nanoscience Initiatives.

[1] J. Frenkel and J. Dorfman, Nature (London) **126**, 274 (1930); C. Kittel, Phys. Rev. **70**, 965 (1946).
[2] C. P. Bean and J. D. Livingstone, J. Appl. Phys. **30**, 1205 (1959); I. S. Jacobs and C. P. Bean, in *Magnetism*, edited by G. T. Rado and H. Suhl (Academic, New York, 1963), Vol. III.
[3] L. Néel, Ann. Geophys. (C.N.R.S.) **5**, 99 (1949); Adv. Phys. **4**, 191 (1955).
[4] A. N. Goldstein, *Hand Book of Nanophase Materials* (Marcel Dekker, New York, 1997).
[5] *Magnetic Properties of Fine Particles*, edited by J. L. Dormann and D. Fiorani (North-Holland, Amsterdam, 1992).
[6] K. M. Unruh and C. L. Chien, in *Nanomaterials: Synthesis, Properties and Applications*, edited by A. S. Edelstein and R. C. Cammarata (Institute of Physics, Bristol, 1996).
[7] A. H. Morrish, *Physical Principles of Magnetism*, (Wiley, New York, 1965).
[8] Steen Mørup and Elisabeth Tronc, Phys. Rev. Lett. **72**, 3278 (1994).
[9] E. P. Wohlfarth, J. Phys. F: Met. Phys. **10**, L241 (1980).
[10] R. Street and J. C. Woolley, Proc. Phys. Soc., London, Sect. A **62**, 562 (1949). Also reviewed in S. Dattagupta, *Relaxation Phenomena in Condensed Matter Physics* (Academic, Orlando, 1987), Chap. XV.
[11] Y. Sun, M. B. Salamon, K. Garnier, and R. S. Averback, Phys. Rev. Lett. **91**, 167206 (2003).
[12] M. Sasaki, P. E. Jonsson, H. Takayama, and P. Nordblad, cond-mat/0311264v2 (unpublished).
[13] J. D. Wright and J. M. Sommerdijk, *Sol-Gel Materials, Chemistry and Applications* (Taylor and Francis, London, 2001).
[14] B. D. Cullity, Elements of x-ray diffraction, 1978.
[15] W. F. Brown, Jr., Phys. Rev. **130**, 1677 (1963); also see W. T. Coffey, Yu. P. Kalmykov, and J. T. Waldron, *The Langevin Equation* (World Scientific, Singapore, 1996).
[16] J. M. Luttinger and L. Tisza, Phys. Rev. **70**, 954 (1946).
[17] See, for instance, A. Abragam, *The Theory of Nuclear Magnetism* (Oxford University Press, London, 1961).
[18] A large body of work on Mössbauer effect in single domain magnetic particles has been carried out by S. Mørup and his group. A recent reference is M. F. Hansen, C. B. Koch, and S. Mørup, Phys. Rev. B **62**, 1124 (2000).
[19] S. Dattagupta, in *Mössbauer Effect: Application to Physics, Chemistry and Biology*, edited by B. V. Thosar, P. K. Iyenger, J. K. Srivastava, and S. C. Bhargava (Elsevier, Amsterdam, 1983).
[20] S. Dattagupta, in *Mössbauer Spectroscopy in Perspectives*, edited by F. J. Berry and D. P. E. Dickson (Cambridge University Press, London, New York, 1986); Hyperfine Interact. **49**, 253 (1989).
[21] Mössbauer data for the *noninteracting* case have been reported by us earlier: S. Chakraverty, K. Mandal, S. Chatterjee, and S. Kumar, Indian J. Phys., A **78A**, 177 (2004).
[22] M. Blume, in *Hyperfine Structure and Nuclear Radiations*, edited by E. Mathias and D. A. Shirley (North-Holland, Amsterdam, 1968); S. Dattagupta and M. Blume, Phys. Rev. B **10**, 4540 (1974).
[23] I. S. Gradshteyn and I. M. Ryzhik, *Tables of Integrals, Series, and Products*, 6th ed. (Academic, New York, 1980).
[24] A. P. Young, *Spin Glasses and Random Fields* (World Scientific, Singapore, 1987).
[25] K. H. Fischer and J. A. Hertz, *Spin Glasses* (Cambridge University Press, Cambridge, 1991).
[26] See for instance, K. Binder and W. Kinzel, in *Heidelberg Colloquium on Spin Glasses*, edited by J. L. Van Hemmen and I. Morgenstern (Springer-Verlag, Berlin, New York, 1983), p.279 and references therein.
[27] M. Bandyopadhyay, Ph.D. dissertation (unpublished).